Baghdad Science Journal

Volume 22 | Issue 6 Article 5

6-17-2025

Synthesis, Characterization and Studying Mass Spectra and Thermal Analysis for Complexes of Some Metal Ions and Determining their Activity as Antioxidants

Fatimah Al-zahraa SH. H
Department of Chemistry, College of Science for Women, University of Baghdad, Baghdad Iraq,
Fatima.Ali2305m@csw.uobaghdad.edu.iq

Abbas Ali Salih Al-Hamdani
Department of Chemistry, College of Science for Women, University of Baghdad, Baghdad Iraq,
abbasas_chem@csw.uobaghdad.edu.iq

How to Cite this Article

H, Fatimah Al-zahraa SH. and Al-Hamdani, Abbas Ali Salih (2025) "Synthesis, Characterization and Studying Mass Spectra and Thermal Analysis for Complexes of Some Metal Ions and Determining their Activity as Antioxidants," *Baghdad Science Journal*: Vol. 22: Iss. 6, Article 5.
DOI: https://doi.org/10.21123/2411-7986.4955

BAGHDAD SCIENCE JOURNAL 2025;22(6):1785–1800

RESEARCH ARTICLE

Synthesis, Characterization and Studying Mass Spectra and Thermal Analysis for Complexes of Some Metal Ions and Determining their Activity as Antioxidants

Fatimah Al-zahraa SH. H *, Abbas Ali Salih Al-Hamdani

Department of Chemistry, College of Science for Women, University of Baghdad, Baghdad Iraq

ABSTRACT

The new azo dye was prepared from the reaction of the diazonium salt derived from 3-aminophenol with 2-hydroxyquinoline, then it was used to prepare a series of complexes with the chlorides of cobalt, chromium, copper, nickel, platinum, palladium and ammonium molybdate. The ligand was identified by a proton and carbon nuclear magnetic resonance spectroscopy, and the compounds were collected. The prepared materials were subjected to infrared, ultraviolet-visible, and mass spectrometry, as well as thermogravimetric analysis, differential calorimetry, and elemental analysis. Conductivity, magnetic susceptibility, metal content, and chlorine content of the complexes were also measured. The results showed that the ligand behaves in a trigonal behavior, and the proposed formula for it was correct, and that the complexes gave tetrahedral and octahedral shapes, except for palladium, square planar shape was given. The results also showed that the complexes contain water within the coordination field and that all of them are non-electrolytes. The dyeused the complexes prepared from it to determine their ability to inhibit free radicals by measuring their ability as antioxidants using DPPH as a free radical and ascorbic acid as a standard substance, and determining the value of IC_{50}, as it was found that the ligand had a high ability to inhibit free radicals, and the ability to inhibit the complexes varied according to the value of IC_{50}. The results are as follows (H_2L > Ascorbic acid > Cu-complex > Mo-complex > Pt-complex > Ni-complex > Pd-complex).

Keywords: Antioxidant, Azo complexes, 3-aminophenol, 2-hydroxyquinoline, Thermodynamic parameter

Introduction

Azo compounds are a very important class of chemical compounds that have received much attention in scientific research. They are highly colorful and have been used as dyes for a long time.[1] Moreover, they have been widely studied due to their excellent thermal and optical properties in applications such as optical recording medium, inkjet printing and light fast dyes in oil solution.[2] Among the biological functions of azo compounds, are antioxidants, which are known as organic or inorganic substances that fight free radicals in the body, and prevent or slow cell damage resulting from free radicals and unstable molecules in the body.[3–5] Antioxidants play a role in fighting the signs of aging, and they also have an important role in strengthening the body's immunity. These classes of compounds can be added to foods to increase their shelf life through a process called delayed lipid peroxidation.[6] Natural and chemical sources may contain these antioxidant compounds. 2, 2-Diphenyl-1-picrylhydrazyl (DPPH) tests have been widely applied to antioxidant activity screening because this class of compounds can accommodate many samples tested in a short time and is sensitive to detect active ingredients at low concentrations.[7,8]

Received 3 October 2023; revised 5 March 2024; accepted 7 March 2024.

* Corresponding author.
E-mail addresses: Fatima.Ali2305m@csw.uobaghdad.edu.iq (F. Al-zahraa SH. H), abbasas_chem@csw.uobaghdad.edu.iq (A. Ali Salih Al-Hamdani).

https://doi.org/10.21123/2411-7986.4955

When DPPH radicals encounter substances containing donated protons such as antioxidants, they will be scavenged and absorption reduced.[9]

This research aims to create new complexes of the metal ions Cr^{+3}, Co^{+2}, Ni^{+2}, Cu^{+2}, Pd^{+2}, Pt^{+4} and Mo^{+6} using the azo ligand H_2L. In addition to characterization with spectroscopic analysis, thermal stability and thermal decomposition which were studied using DSC and TGA curves, and the antioxidant activity of these compounds was assessed against the DPPH radical and compared to that of a reference natural antioxidant ascorbic acid.

Materials and methods

The trading providers (SigmaAldrich, Merck, and others) have provided the materials. To obtain (C.H.N), the Perkin-Elmer model EA/2400, singleV_3O, has been used. Using a gravimetric-approach, mineral-ions have been identified as M-O. Using a conductometer W-T-W, 25 °C, molar conductivity has been estimated 1×10^{-3} M. Solvents have been used, such as DMSO. Mass spectrometry (MS) Q-P-50-A-D-I Analysis Shimadzu QP(E170Ev)-2010-Pluss spectrometer has been used to collect mass spectra for various compounds. The UV-1800 Shimadzu Spectrophotometer was used to get the UV-visibleabsorption spectra. The UV-visible absorption spectra were obtained using a UV-1800 Shimadzu Spectrophotometer. The ^1H- and ^{13}C-NMR spectra were obtained using the Brucker (400 MHz) Spectrometer. The Fourier Transform Infrared (FTIR) spectra were investigated using the IR Prestige-21, and the instruments employed were the Bruker 4000–500 cm^{-1} and the Shimadzu 4000–200 cm^{-1}.Metals were identified using a Shimadzu (F.A.A) 680 G atomic clock. Magnetic properties were used with the balancing susceptibility model MSR-MKI. All earlier types of thermal analysis employed Perkin-Elmer Pyris Diamond DSC/TGA.

Synthesis of azo dye ligand: [2-[(3-hydroxyphenyl)diazinyl]-1, 2-benzothiazol-3(2H)-one 1, 1-dioxide]

3-Aminophenol (1 g, 0.008 mmol) has been dissolved in(2 mlHCl, 15 ml of ethanol, and 10 ml of distilled water) under refrigeration, at 0 to 5 °C. Reducing the temperature to 5 °C, amounts (10%, 1 g, 14.49 mmol) $NaNO_2$ were added gradually. The reaction has been stirred for approximately 45 minutes, (1.16 g, 0.008 mmol) of 2-hydroxyquinoline dissolved in 15 ml of ethanol were added. A change to a dark colored solution was observed after stirring for 30 minutes to carry out the reaction. This product was collected after being filtered and dried. Its melting point was 253–255 °C and brown precipitate, and its yield was 87%. Scheme 1 shows the formation of the ligand azo dye.

Preparation of metallic metal ions complexes

The metal salt (1 mmol)[$CrCl_3$. $6H_2O$ 0.1 g, $NiCl_2$. $6H_2O$0.1 g, $CoCl_2$. $6H_2O$0. 1 g, $CuCl_2$. $2H_2O$ 0.07 g, H_2PtCl_6. $6H_2O$ 0.2 g, $(NH_4)_2MoO_4$ 0.08 g and $PdCl_2$ 0.7 g] was dissolved in 10 ml of ethanol. (15 ml) from Azo ligand H_2L (0.1 g, 1 mmol) was added drop by drop. The end product was heated and refluxed for two hours at a temperature of 40 °C. By briefly submerging the solid complexes in hot ethanol, any unreacted components were separated from them and eliminated. We gathered, dried, and weighed the complexes. The creation of the metal ions complexes is depicted in Scheme 1.

Results and discussion

Physical and analytical data for ligand(H_2L) and the complexes synthesized

Metal salts and ligand reacted to produce the synthetic compounds are shown in Scheme 1. The findings of the elemental analysis showed that all compounds have a 1:1 M:Lstoichiometry. The results of the elemental analysis agreed with those of the theoretical calculations, and all complexes are non-electrolytes, as shown in Table 1.

NMR-nuclear magnetic resonance

The ^1H-NMR and ^{13}C-NMR spectrum of new azo, which can be seen in Fig. 1 demonstrates the chemical shifts of these spectra. ^1H-NMR(DMSO-$d_6$ppm) 2.45 ppm, (2H, s), NH, 7.26 ppm (1H, s), C-H aromatic beside OH 7.71–7.72 ppm (1H, d), C-Haromaticbeside N=N 8.10–8.11 ppm (1H, d), OH11. 66–11.68 ppm (2H, d) respectively. ^{13}C-NMR: 127.48 (C1) 148.96 (C2), 118.20 (C3) 145.0 (C4), 157.23 (C5), 169.75 (C6), 132–21 (C7) 165.30(C8), 137.27 (C9), 166.90 (C10) 155.15 (C11), 122.24 (C12), 178–10 (C13), 181.97 (C14) 189.75 (C15) respectively.[10–12]

FT-IR spectroscopy

The infrared spectra of ligand H_2L and its metal complexes were recorded with have been compiled Cr^{+3}, Co^{+2}, Ni^{+2}, Cu^{+2}, Pd^{+2}, Pt^{+4} and Mo^{+6} and the data has been organized in Table 2. The ligand

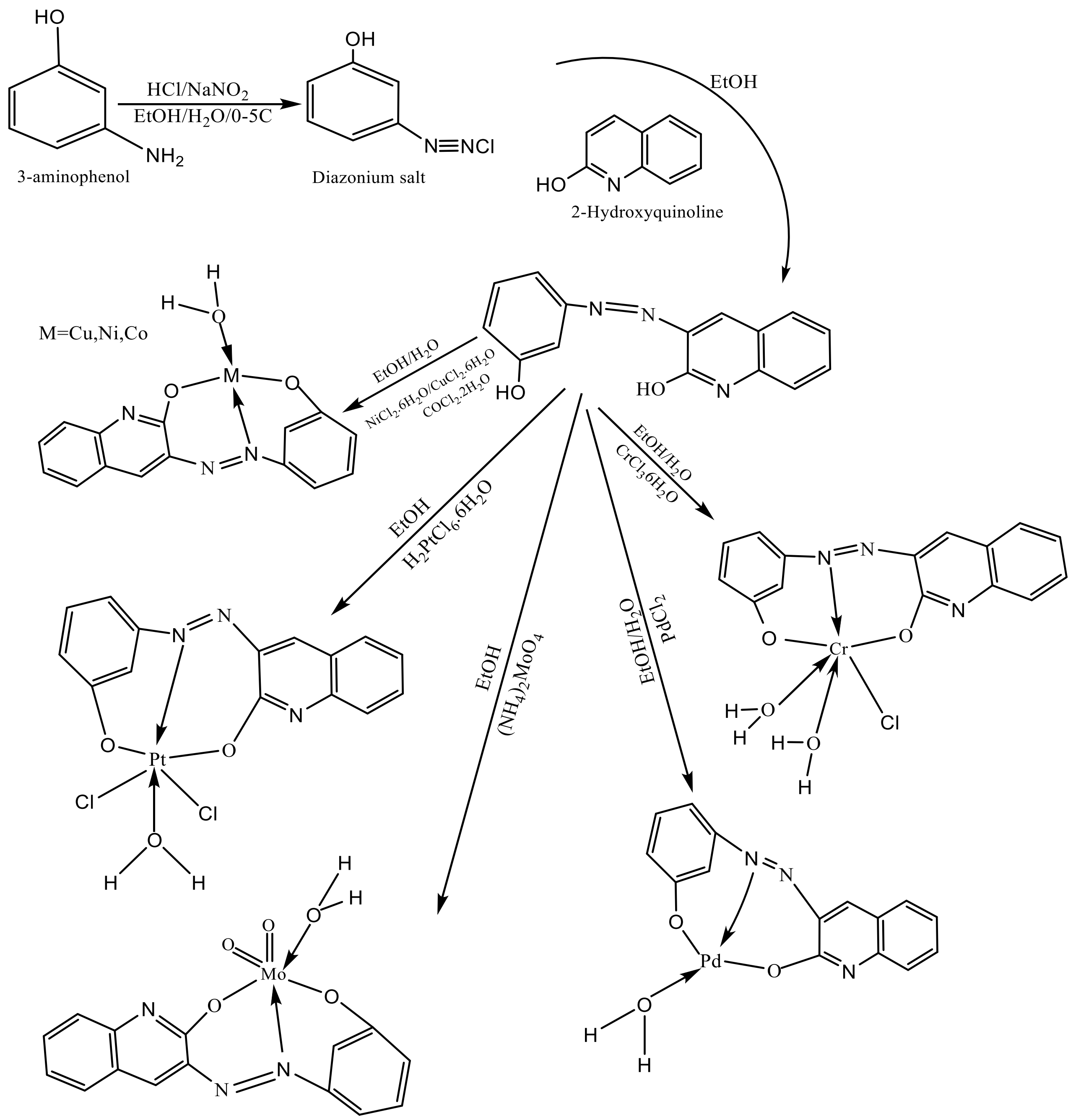

Scheme 1. Synthesis of azo dye ligand and metal complexes.

showed bands at 3477, 3167, (1546–1600), and 1257 cm^{-1} that were ascribed to the ν(OH) phenolic, ν(C-H) aromatic, ν(C=C), and ν(C-O). The infrared spectrum of the ligand showed a medium intensity stretch band at frequency 1352 cm^{-1}, which was attributed to the vibration frequencies of the doublebond N=N. After this, following this, the IR spectra of all the compounds created showed that the azo-dye ligand coupled to metal ions through two sites: the oxygen site via deprotonating of the phenolic group and the nitrogen site of the azo group. New bands belonging to (M-N) appeared at (570, 567, 524, 535, 503, 466 and 525) cm^{-1} for the Cr^{+3}, Pt^{+4}, Cu^{+2}, Mo^{+6}, Co^{+2}, Ni^{+2} and Pd^{+2} complexes, respectively, (M-O) at (532, 482, 462, 485, 460, 428 and 463) cm^{-1} for the complexes Cr^{+3}, Pt^{+4}, Cu^{+2}, Mo^{+6}, Co^{+2}, Ni^{+2} and Pd^{+2} respectively, (M-Cl) at (400, 390) cm^{-1} for the complexes of Cr^{+3} and Pt^{+4} respectively, the spectrum has been discussed according to the reference standard.[11–13]

Table 1. Some elemental physical characteristics investigations of ligand and complexes.

	C%	H%	N%	M%	Cl%	mp ºC	
Formula Molecular weight	Calculated (found)						Conductivity in DMSOcm^2 Ω^{-1}mol^{-1}
$C_{15}H_{11}N_3O_2$	67.09	3.72	16.81				
265.27	67.92	4.18	15.84			253–255	
$C_{15}H_{13}N_3O_4ClCr$	46.59	3.39	10.87	13.45	9.17		9
386.73	45.88	2.55	11.45	12.41	10.01	235–237	
$C_{15}H_{11}N_3O_3Co$	52.96	3.26	12.35	17.32			14
340.20	53.30	3.32	13.22	17.21		177–179	
$C_{15}H_{11}N_3O_3Ni$	52.99	3.26	12.36	17.26			10
339.96	53.48	2.89	13.51	16.60		244–247	
$C_{15}H_{11}N_3O_3Cu$	52.25	3.22	12.19	18.43			9
344.81	51.44	3.88	13.42	17.45		200–202	
$C_{15}H_{11}N_3O_3Pd$	46.47	2.86	10.84	27.45			13
387.69	45.65	3.21	11.69	27.22		301–305	
$C_{15}H_{11}N_3O_3PtCl_2$	32.92	2.03	7.68	35.65	12.96		11
547.25	33.02	3.01	8.66	36.49	13.58	288–289	
$C_{15}H_{11}N_3O_5Mo$	44.03	2.71	10.27	23.45			19
409.21	43.81	3.09	11.19	24.25		189–191	

Table 2. The IR spectra bands (cm^{-1}) of compounds.

Compound	ν (H_2O) aqua	ν(C-H) aromatic	ν (C-O)	ν (N=N)	Other bands
H_2L	–	3167	1257	1352	3477(OH-Phenol)
[Mo(L)O_2(H_2O)]	3352, 1620 840, 682	3146	1143	1408	535(Mo-N) 485(Mo-O) 958(Mo=O)
[Co(L)H_2O]	3421, 1645 835, 536	3182–2993	1147	1415	503(Co-N) 460(Co-O)
[Ni(L)H_2O]	3392, 1616 833, 582	3100	1147	1409	466(Ni-N) 428(Ni-O)
[Cu(L)H_2O]	3377, 1647 835, 756	3167	1217	1409	524.64(Cu-N) 462.92(Cu-O)
[Pd(L)H_2O]	3415, 1622 852	3104	1222	1411	525.60(Pt-N) 463.90(Pt-O)
[Pt(L)H_2OCl_2]	3334, 1622 829, 682	3148	1227	1406	567(Pt-N), 482(Pt-O)390(Pt-Cl)
[Cr(L)(H_2O)$_2$Cl]	3560, 1595 840, 682	3190–3100	1298	1408	532(Cr-O), 570(Cr-N)400(Cr-Cl)

UV-VisSpectra and magnetic susceptibility

The electronic spectrum for ligand (H_2L) exhibits strong absorbance at (275 nm, 36363.64 cm^{-1}) ascribed to the $\pi \rightarrow \pi^*$ transition and peak at (350 nm, 28571.43 cm^{-1}) attributed to the $n \rightarrow \pi^*$ transition a peak with a high intensity band formed with absorption maxima. The electronic transition of Cr^{+3} complex is which depicts a peak of (315, 420, 630 and 780) nm assigned to $\pi \rightarrow \pi^*$, $n \rightarrow \pi^*$, C.T L $\rightarrow$ M $^6A_1g \rightarrow {}^4Eg(G)$ and $^6A_1g \rightarrow {}^4T_2g(G)$ respectively, μ_{eff} = 3.771 B.M, which is an indicative of anoctahedral geometry.[13,14] The electronic spectrum of the Co^{+2} compound was studied, exhibits peak of (285, 310, 415 and 685) nm assigned to $\pi \rightarrow \pi^*$, $n \rightarrow \pi^*$, C.T L $\rightarrow$ M and $^6A_1g \rightarrow {}^4Eg(G)$ respectively, μ_{eff} = 3.896 B.M, which is an indicative of a tetrahedralgeometry. The electronic transition of Ni^{+2} complex is which depicts a peak of 320, 475, 490 and 625 nm assigned to $\pi \rightarrow \pi^*$, $n \rightarrow \pi^*$, $^3T_{1(F)} \rightarrow {}^3A_{2(F)}$ and $^3T_{1(F)} \rightarrow {}^3T_{1(P)}$ respectively, μ_{eff} = 2.853 B.M, which is an indicative of a Tetrahedral geometry. The electronic transition of Cu^{+2} complex is which depicts a peak of 215 and 405 nm assigned to $\pi \rightarrow \pi^*$, $n \rightarrow \pi^*$ respectively, μ_{eff} = 1.763 B.M, which is an indicative of a tetrahedralgeometry.[15] The electronic transition of Mo^{+6} complex is which depicts a peak of (278, 325 and 398) nm assigned to $\pi \rightarrow \pi^*$, $n \rightarrow \pi^*$ and C.T M $\rightarrow$ L respectively, which is an indicative of an octahedralgeometry. The electronic transition of Pd^{+2} complex is which depicts a peak of 298, 415, 655 and 795 nm assigned to $\pi \rightarrow \pi^*$, $n \rightarrow \pi^*$, C.T M $\rightarrow$ L, $^1A_1g \rightarrow {}^1B_1g$ and $^1A_1g \rightarrow {}^1A_2g$ respectively, which is an indicative of a square planargeometry. The electronic transition of Pt^{+4} complex which depicts a peak of 255, 305, 412, 580, 610 and 650 nm assigned to $\pi \rightarrow \pi^*$, $n \rightarrow \pi^*$, $^1A_1g \rightarrow {}^1T_1g$,$^1A_1g \rightarrow {}^1T_2g$ and $^1A_1g \rightarrow {}^1T_3g$ respectively, which is an indicative

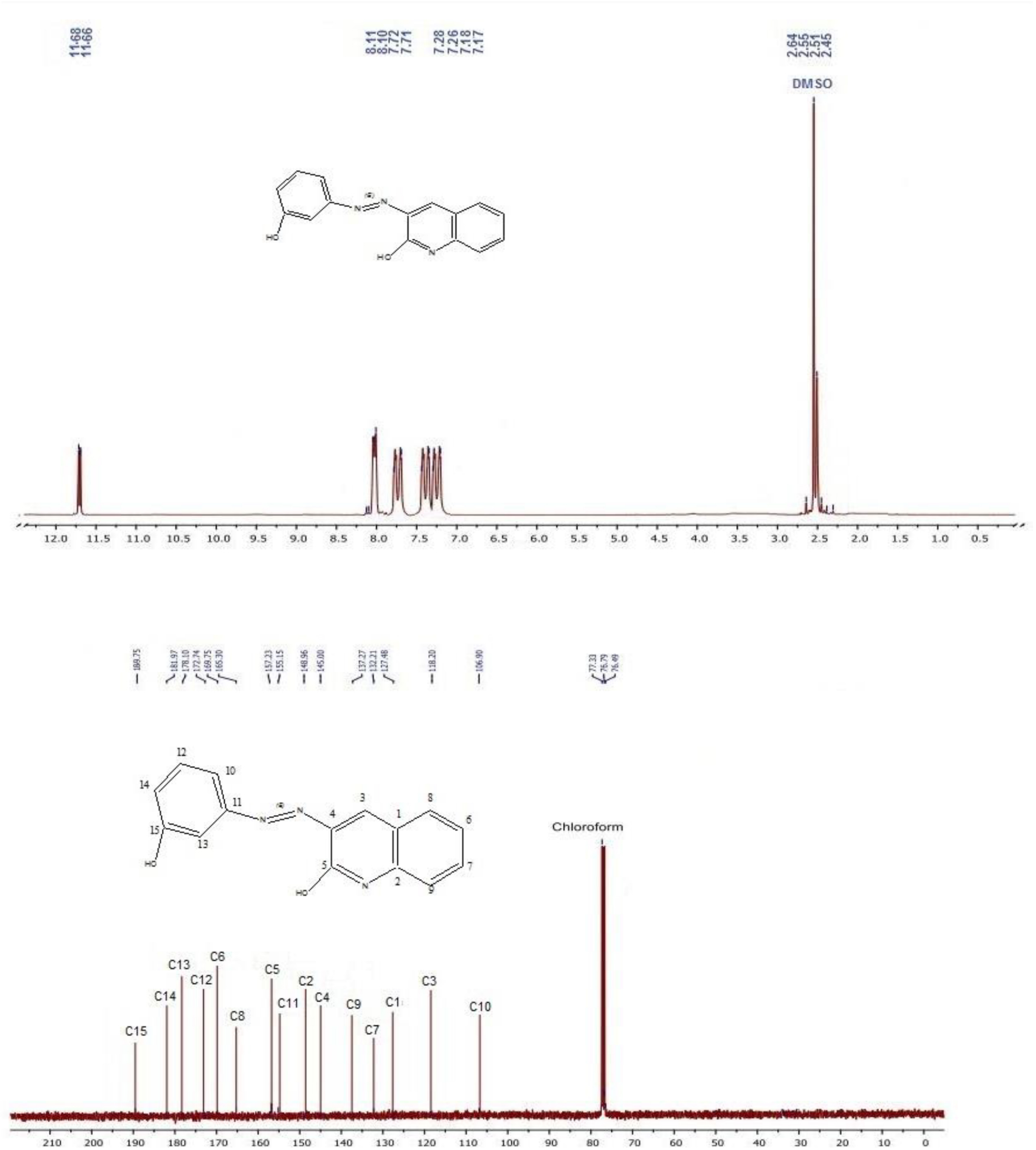

Fig. 1. 1H and ^{13}C-NMR spectra of ligand (H_2L).

of anoctahedral geometryas in Table 3, the spectrum has been discussed according to the reference standard.[16,17]

LC-mass measurements

One of the most crucial methods for characterizing the ligand (H_2L) and some products was the LC-Mass spectrum testing. This method is supplementary to the other methods that estimate the molecular weight of the chemical using the relationship the fragmentation pattern and the extract mass for each pattern are shown in Scheme 2 mass information for the ligand. The fragment's molecular ion peak $[M]^+$ is easily visible $C_{15}H_{10}N_3O^+$ and its relative abundance about 67%, in addition to other abundances for the rest of peaks including $C_{15}H_{10}N_3{}^+$, $C_9H_6N^+$ and $C_6H_5N_2{}^+$ corresponded the next abundances:

Table 3. Electronic spectral dataof the compounds and magnetic moment.

Compound	λ nm	ύcm^{-1}	Abs	ε_{max} L mol^{-1}cm^{-1}	Assignment	μ_{eff} (B.M)	Hybridization	Distribution
Ligand H_2L	275	36363.64	1.89	1890	$\pi \rightarrow \pi^*$			
	350	28571.43	2.13	2130	n$\rightarrow \pi^*$			
$[Cr(L)(H_2O)_2Cl]$ Octahedral	315	31746.03	0.510	510	$\pi \rightarrow \pi^*$	3.771	$d^2\ sp^3$	$T_2g^3\ eg^0$
	420	23809.52	0.023	485	n$\rightarrow \pi^*$ + C.T			
	630	15873.01	0.485	23	L$\rightarrow$M			
	780	12820.51	0.012	12	$^6A_1g\rightarrow{}^4Eg_{(G)}$ $^6A_1g\rightarrow{}^4T_2g_{(G)}$			
$[Ni(L)H_2O]$ Tetrahedral	320	31250	0.825	825	$\pi \rightarrow \pi^*$	2.896	Sp^3	$e^4t_2{}^4$
	475	21052.63	0.490	490	n$\rightarrow \pi^*$			
	490	20408.16	0.497	215	$^3T_{1(F)} \rightarrow {}^3A_{2(F)}$			
	625	16000	0.215	497	$^3T_{1(F)} \rightarrow {}^3T_{1(P)}$			
$[Mo(L)O_2(H_2O)]$ Octahedral	278	35971.22	2.123	2123	$\pi \rightarrow \pi^*$	dia	$sp^3\ d^2$	$T_2g^0\ eg^0$
	325	30769.23	1.982	1982	n$\rightarrow \pi^*$			
	398	25125.62	0.098	982	C.T L$\rightarrow$M			
$[Cu(L)H_2O]$ Tetrahedral	251	39840.63	1.995	1995	$\pi \rightarrow \pi^*$	1.763	Sp^3	$e^4t_2{}^5$
	405	24691.35	0.073	735	n$\rightarrow \pi^*$			
$[Co(L)H_2O]$ Tetrahedral	285	35087.71	1.250	1250	$\pi \rightarrow \pi^*$	3.896	Sp^3	$e^4t_2{}^3$
	310	32258.06	1.490	1490	n$\rightarrow \pi^*$			
	415	24096.38	0.321	321	C.T L$\rightarrow$M			
	685	14598.54	0.145	145	$^6A_1g\rightarrow{}^4Eg_{(G)}$			
$[Pd(L)H_2O]$ Square Planar	298	33557.04	0.512	512	$\pi \rightarrow \pi^*$	dia	dsp^2	$T_2g^6eg^2$
	415	24096.38	0.585	585	n$\rightarrow \pi^*$+C.T			
	655	15267.17	0.090	90	M$\rightarrow$L			
	795	12578.61	0.085	85	$^1A_1g \rightarrow {}^1B_1g$ $^1A_1g \rightarrow {}^1A_2g$			
$[Pt(L)H_2OCl_2]$ Octahedral	255	39215.68	1.730	1730	$\pi \rightarrow \pi^*$	dia	d^2sp^3	$T_2g^6\ eg^0$
	305	32786.88	1.625	1625	n$\rightarrow \pi^*$			
	412	24271.84	0.495	495	C.T L$\rightarrow$M			
	580	17241.37	0.021	21	$^1A_1g\rightarrow{}^1T_1g$			
	610	16393.44	0.017	17	$^1A_1g\rightarrow{}^1T_2g$			
	650	15384.61	0.011	11	$^1A_1g\rightarrow{}^1T_3g$			

dia= diamagnetic.

45%, 32%, 88% respectively. For $[Cr(L)Cl(H_2O)_2]$, Scheme 2, we can also detect the molecular ion peak (M^+) at 386.73 m/z with relative abundance 20% and next pattern: $C_{15}H_9ClCrN_3O_2{}^+$, $C_{15}H_9CrN_3O_2{}^+$, $C_{15}H_9CrN_3O^+$, $C_9H_5CrN_3O^{+\cdot}$, $C_6H_4{}^{\cdot+}$, $C_2CrN_2O^{\cdot+}$, $C_7H_5N^{\cdot+}$ which corresponded to 350.70 m/z, 315.25 m/z, 299.25 m/z, 223.15 m/z and 76.10 m/z, 120.03 m/z, 103.12 m/z respectively, corresponded the next abundances: 55%, 40%, 35%, 25%, 75%, 47%, 85% respectively.[16] For $[Co(L)H_2O]$, Scheme 2, we can also detect the molecular ion peak (M^+) at 340.20 m/z with relative abundance 7% and next pattern: $C_{15}H_8N_3O_2Co^+$, $C_{15}H_8CoN_3O^{+\cdot}$, $C_9H_4CoNO^{+\cdot}$, $C_6H_4N_2{}^{+\cdot}$ which corresponded to 321.18 m/z, 305.18 m/z, 201.07 m/z, 104.11 m/z respectively, corresponded the next abundances: 15%, 65%, 45%, 78% respectively. For $[Pd(L)H_2O]$, Scheme 2, we can also detect the molecular ion peak (M^+) at 387.69 m/z with relative abundance 8% and next pattern: $C_{15}H_8N_3O_2Pd^+$, $C_{15}H_8PdN_3O^{\cdot+}$, $C_{15}H_8PdN_2O^{\cdot+}$, $C_9H_3PdN_2O^{\cdot+}$, $C_6H_5{}^+$ which corresponded to: 368.66 m/z, 352.66 m/z, 338.66 m/z, 261.05 m/z, 77.10 m/z respectively, corresponded the next abundances: 20%, 45%, 40%, 38%, 32% respectively.[17] For $[Pt(L)(Cl)_2H_2O]$, we can also detect the molecular ion peak (M^+) at 547.25 m/z with relative abundance 17% and next pattern: $C_{15}H_8Cl_2N_3O_2Pt^+$, $C_{15}H_8ClN_3O_2Pt^+$, $C_{15}H_8N_3OPt^{\cdot+}$, $C_9H_4N_3Pt^{+\cdot}$, $C_9H_3N^{+\cdot}$, N_2Pt^+, $C_6H_4O^{+\cdot}$ which corresponded to: 528.23 m/z, 492.77 m/z, 441.32 m/z, 217.69 m/z, 125.13 m/z, 223.09 m/z, 92.10 m/z respectively, corresponded the next abundances: 12%, 45%, 67%, 65%, 48%, 62%, 49% respectively. For $[Ni(L)H_2O]$, we can also detect the molecular ion peak (M^+) at 339.96 m/z with relative abundance 5% and next pattern: $C_{15}H_8N_3O_2Ni^+$, $C_{15}H_8N_3NiO^{+\cdot}$, $C_9H_4N_3Ni^+$, $C_9H_3N^{+\cdot}$, $C_6H_4O^+$, N_2Ni^+ respectively, corresponded the next abundances: 320.94 m/z, 304.94 m/z, 212.84 m/z, 125.13 m/z, 92.10 m/z, 86.71 m/z respectively, corresponded the next abundances: 35%, 44%, 62%, 48%, 78%, 33% respectively. For $[Cu(L)H_2O]$, we can also detect the molecular ion peak (M^+) at 344.81 m/z with relative abundance 7% and next pattern: $C_{15}H_8N_3O_2Cu^+$, $C_{15}H_8CuO^{+\cdot}$, $C_9H_4N_3Cu^{+\cdot}$, $C_9H_3N^{+\cdot}$, $C_6H_4O^{+\cdot}$, N_2Cu^+ respectively,

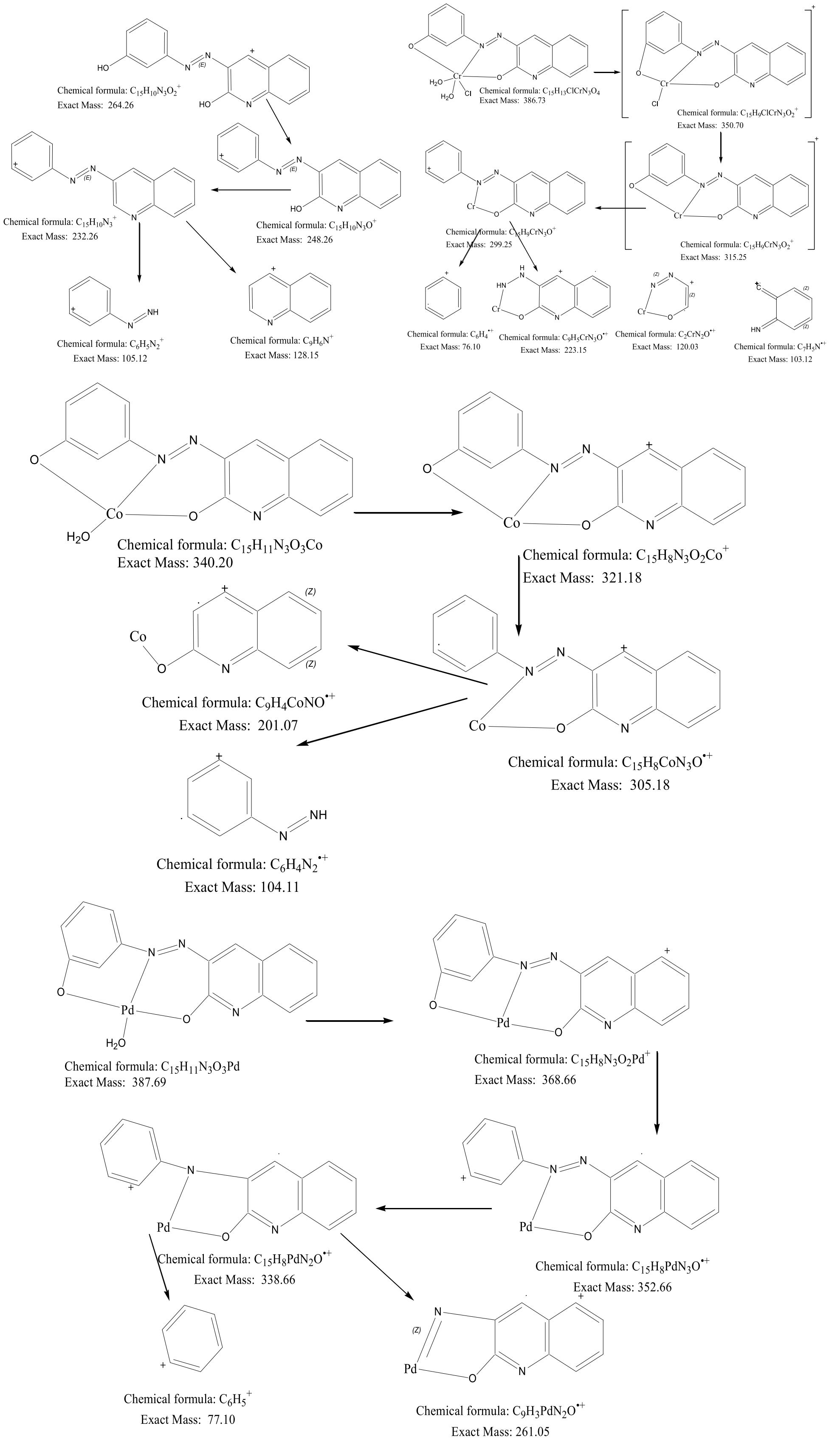

Scheme 2. Pattern of Fragmentation of compounds.

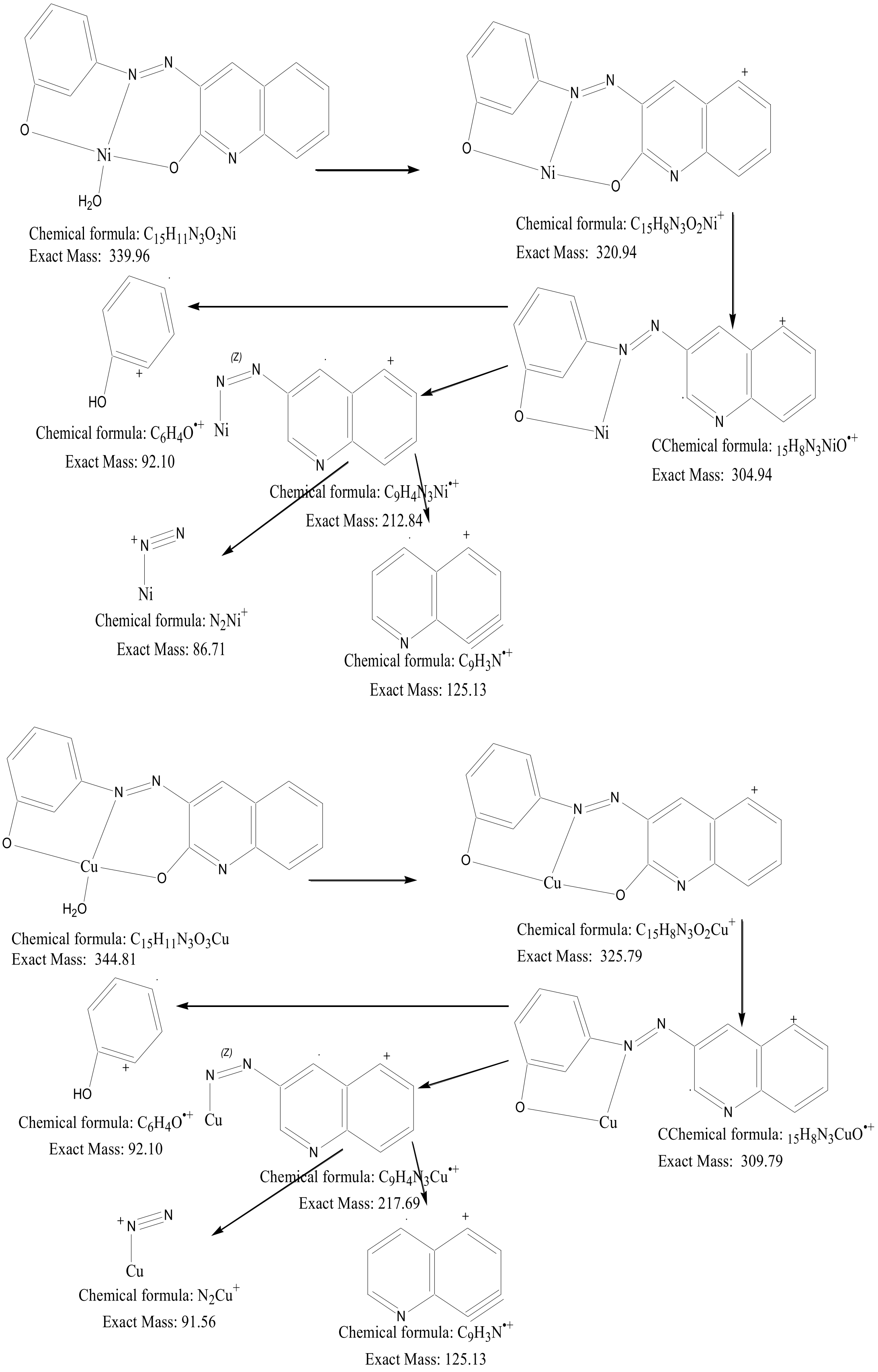

Scheme 2. Continued.

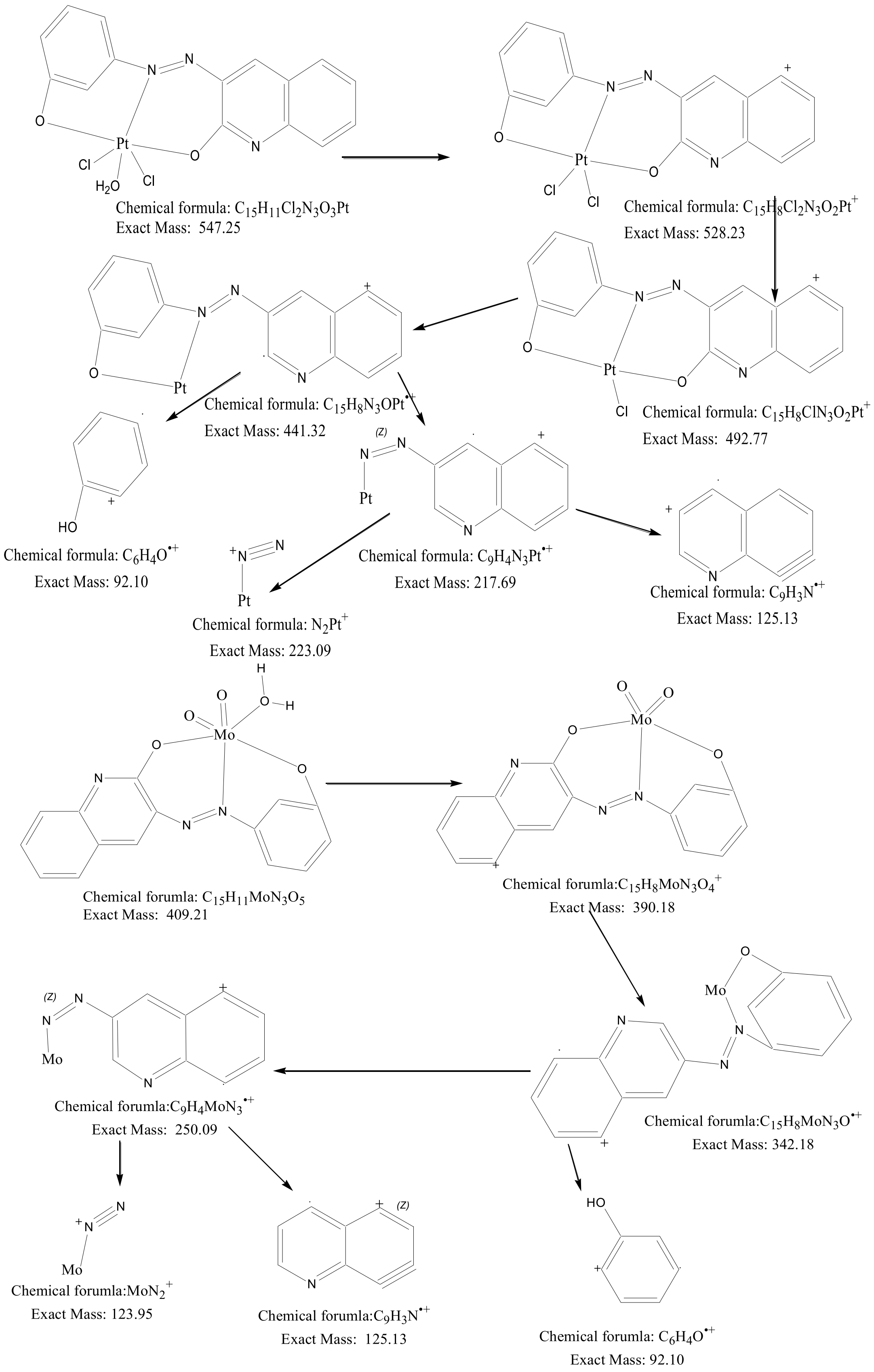

Scheme 2. Continued.

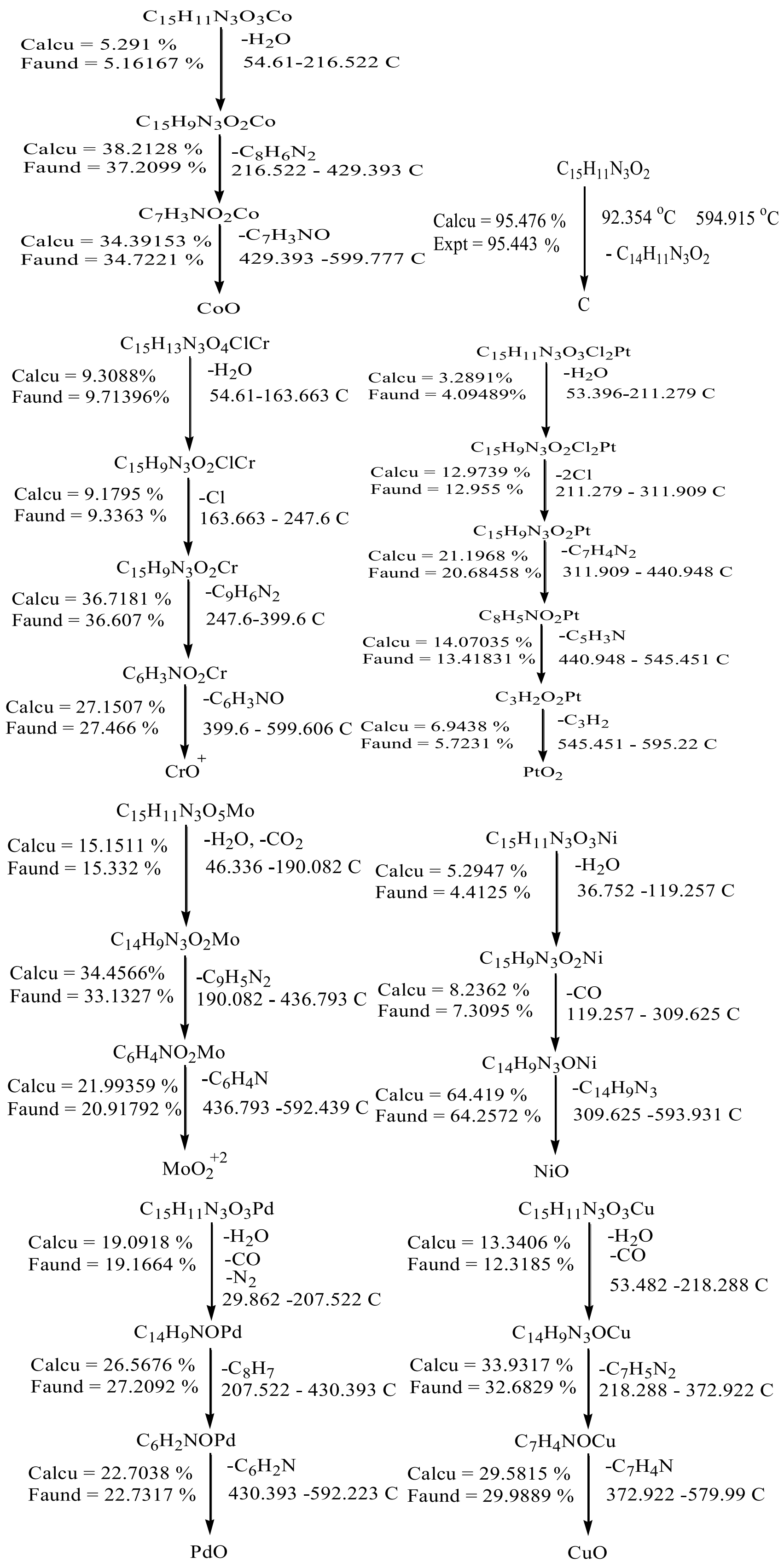

Scheme 3. Tentative decomposition reaction of ligand and complex.

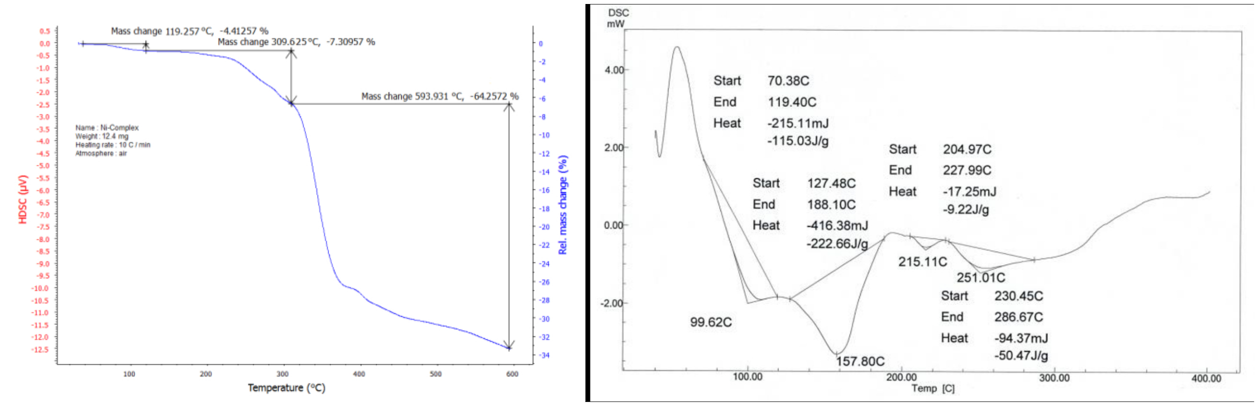

Fig. 2. TGA and DSC curve of Ni-complex.

Table 4. TGA data of the ligand H_2Landsome complexes.

Complex	Step	$T_{i/°C}$	$T_{f/°C}$	Weight mass loss%	Reaction
Ligand	1	92.354 °C	594.915 °C	Calc Found 95.476%95.443%	-$C_{14}H_{11}N_3O_2$ C
Calculated:	95.476%	Final=	4.524%	Estimated: 95.443% Final= 4.557%	
Ni-complex	1	36.752 °C	119.257 °C	5.2947% 4.4125%	-H_2O
	2	119.257 °C	309.625 °C	8.2362% 7.3095%	-CO
	3	309.625 °C	593.931 °C	64.419%64.2572%	-$C_{14}H_9N_3$ NiO
Calculated:	77.95%	Final=	22.05%	Estimated:75.9792% Final=24.02%	
Cu-complex	1	53.482 °C	218.288 °C	13.3406%12.3185%	-H_2O, -CO
	2	218.288 °C	327.922 °C	33.9317%32.6829%	-$C_7H_5N_2$
	3	327.922 °C	579.99 °C	29.5815%29.9889%	-C_7H_5N
					CuO
Calculated:	76.85%	Final=	23.14%	Estimated:74.99% Final=25.01%	
Pd-complex	1	29.862 °C	207.522 °C	19.0918%19.1664%	-H_2O, -CO, -N_2
	2	207.522 °C	430.393 °C	26.5676%27.2092%	-C_8H_7
	3	430.393 °C	592.223 °C	22.7038%22.7317%	-C_6H_2N
					PdO
Calculated:	68.29%	Final=	31.708%	Estimated:69.12% Final=30.892%	
Co-complex	1	54.61 °C	216.522 °C	5.219%5.16167%	-H_2O
	2	216.522 °C	429.393 °C	38.2128%37.2099%	-$C_8H_6N_2$
	3	429.393 °C	599.777 °C	34.39153%34.7221%	-C_7H_3NO
					CoO
Calculated:	77.89%	Final=	22.10%	Estimated:77.093% Final=22.91%	
Mo-complex	1	46.336 °C	190.082 °C	15.1511%15.332%	-H_2O, -CO_2
	2	190.082 °C	436.793 °C	34.4566%33.1327%	-$C_9H_5N_2$
	3	436.793 °C	592.439 °C	21.99326%20.91792%	-C_6H_4N
					$MoO_2{}^{+2}$
Calculated:	71.60%	Final=	28.39%	Estimated:69.38% Final=30.62%	
Cr-complex	1	54.61 °C	163.663 °C	9.3088%9.71396%	-H_2O
	2	163.663 °C	247.6 °C	9.1795%9.3363%	-Cl
	3	247.6 °C	3399.6 °C	36.7181%36.607%	-$C_9H_6N_2$
	4	3399.6 °C	599.606 °C	27.1507%27.466%	-C_6H_3NO
					CrO^+
Calculated:	82.357%	Final=	17.6429%	Estimated: 83.123% Final=16.877%	
Pt-complex	1	53.396 °C	211.279 °C	3.2891%4.09489%	-H_2O
	2	211.279 °C	3.11909 °C	12.9739%12.955%	-2Cl
	3	3.11909 °C	440.948 °C	21.1968%20.68458%	-$C_7H_4N_2$
	4	440.948 °C	545.451 °C	14.07035%13.41831%	-C_5H_3N
	5	545.451 °C	595.22 °C	6.9438%5.7231%	-C_3H_2
					PtO_2
Calculated:	58.474%	Final=	41.526%	Estimated:56.8758% Final=43.124%	

corresponded the next abundances: 325.79 m/z, 309.79 m/z, 217.69 m/z, 125.13 m/z, 92.10 m/z, 91.56 m/z respectively, corresponded the next abundances: 40%, 58%, 73%, 31%, 82% respectively.[18] For $[Mo(L)O_2(H_2O)]$, we can also detect the molecular ion peak (M^+) at 409.21 m/z with relative abundance 5% and next pattern: $C_{15}H_8N_3O_4Mo^+$, $C_{15}H_8N_3MoO^{+\cdot}$, $C_9H_4N_3Mo^{+\cdot}$, $C_9H_3N^{+\cdot}$, $C_6H_4O^{+\cdot}$,

Table 5. Thermal decomposition DSC of Ligand and some complexes.

Compound	$T_{i/°C}$	$T_{f/°C}$	Maximum temperature point °C	ΔH J/g	ΔS J	ΔG J	Type
H_2L	67.21	128.67	97.27	-89.78	-1.4608	52.31	endothermic
$[Cr(L)(H_2O)_2Cl]$	70.38	121.40	51.02	-115.03	-2.254	109.51	endothermic
	127.48	188.10	60.62	-216.66	-3.574	347.31	endothermic
	216.97	227.59	10.62	-16.22	-1.527	312.25	endothermic
	230.45	267.67	37.22	-86.47	-2.323	496.62	endothermic
$[Co(L)H_2O]$	41.08	106.52	65.44	-37.45	-0.572	0.75	endothermic
	127.85	172.88	45.03	-17.08	-0.379	40.06	endothermic
	182.36	196.21	13.85	-1.19	-0.085	14.938	endothermic
	218.64	305.41	86.77	238.78	2.751	-462.09	exothermic
$[Ni(L)H_2O]$	70.38	119.40	49.02	-115.03	-2.346	118.67	endothermic
	127.48	188.10	60.62	-222.66	-3.673	356.93	endothermic
	204.97	227.99	23.02	-9.22	-0.400	76.824	endothermic
	230.45	286.67	56.22	-50.47	-0.897	174.68	endothermic
$[Cu(L)H_2O]$	387.95	395.87	7.92	-3.87	-0.4886	189.59	endothermic
$[Pd(L)H_2O]$	105.94	112.21	6.27	-2.19	-0.3492	37.416	endothermic
	153.16	157.31	4.15	-0.59	-0.1421	22.05	endothermic
	314.19	319.19	5	-3.44	-0.668	206.09	endothermic
$[Pt(L)H_2OCl_2]$	70.38	115.48	45.1	-128.33	-2.845	155.08	endothermic
	127.88	184.10	56.22	-212.66	-3.782	369.01	endothermic
	219.67	227.59	7.92	-15.32	-1.934	394.9	endothermic
	230.95	267.67	36.72	-83.43	-2.272	37	endothermic
$[Mo(L)O_2\ (H_2O)]$	41.08	106.52	65.44	-38.85	-0.593	1.98	endothermic
	128.85	173.88	45.03	-18.08	-0.401	42.78	endothermic
	186.36	198.21	11.85	-1.89	-0.159	28.13	endothermic
	218.64	305.41	86.77	238.78	2.751	-462.09	exothermic

N_2Mo^+ respectively, corresponded the next abundances: 390.18 m/z, 342.18 m/z, 250.09 m/z, 125.13 m/z, 123.95 m/z, 92.10 m/z respectively, corresponded the next abundances: 9%, 33%, 50%, 62%, 17%, 53%, 78% respectively, the spectrum has been deliberated by the established benchmark.[19,20]

Thermal measurements

Data from the thermal analysis are shown in Tables 4 and 5 and Fig. 2 for Ni-complex;tentative decomposition reaction of metal complexes is summarized in Scheme 3. Decomposition stages, temperature ranges, decomposition products, and weight loss complex percentages were computed based on the thermograms, and they showed agreement between their thermal decomposition results and calculated values that validates elementalanalysis results and suggested equation. In this work, it was noted that in the ligand and metal complexes of Cr^{+3}, Co^{+2}, Ni^{+2}, Cu^{+2}, Pd^{+2}, Pt^{+4} and Mo^{+6} the remaining ligand was carbon and the remaining metal oxide. The thermo gravimetric experiments showed that the complexes and ligand separate into (one to three) phases. Using the DCS curve, the thermodynamic parameters ΔH, ΔS, and ΔG were calculatedand the amount of heat for the ligand and complexes was mostly endothermic.[21,22] As for entropy, it is a measure of the amount of randomness and irregularity. A positive value means that the reaction is random and irregular, and negative values mean that the reaction is not random and regular. Most of the complexes have negative values, meaning they are not random and regular. As for the compression free energy, if the values are negative, it means that the reaction is spontaneous at all temperatures, and if it is positive, it means that the reaction is not spontaneous at all temperatures, and complexes in general are mostly positive.[23,24]

Investigation of antioxidant activity

The antioxidant activity of H_2L and its mineral complexes was measured by ascorbic acid and the DPPH assay was used to scavenge free radicals.[25,26] Each sample was first diluted with the same volume of methyl alcohol and then combined with the same volume of concentrated 0.135 mM DPPH solution.[27] After adding the DPPH solution. The samples were kept at room temperature in the dark for 30 minutes.[28] The absorbance of each sample was then determined at 517 nm. The lower for IC_{50} value of the complexes compared to ascorbic acid, the greater their ability to suppress free radicals, as the ligand was the most free radical inhibitor,[29,30] followed byH_2L > Ascorbic acid > $[Cu(L)H_2O]$ > $[Mo(L)O_2\ (H_2O)]$ > $[Pt(L)H_2OCl_2]$ > $[Ni(L)H_2O]$ > $[Pd(L)H_2O]$, as shown in the Table 6.

Table 6. The antioxidant results of ligand and their metal complexes.

Compounds	Concentration μg/ml	PI%	RSA%	$IC_{50}\mu g/ml$
Ascorbic acid	0.374	12.29	87.80	0.021
	0.186	36.75	63.25	
	0.03	58.74	41.26	
LigandH_2L	0.375	18.37	81.63	0.019
	0.186	42.18	57.82	
	0.093	64.17	35.83	
	0.046	77.91	22.09	
$[Pd(L)H_2O]$	0.113	69.48	30.52	1.199
	0.057	84.38	15.62	
	0.028	89.49	10.51	
	0.013	94.38	5.62	
$[Pt(L)H_2OCl_2]$	0.374	36.16	63.14	0.242
	0.186	40.72	59.28	
	0.093	54.48	45.52	
	0.046	63.36	36.64	
$[Ni(L)H_2O]$	0.113	67.48	32.52	1.187
	0.057	82.38	17.62	
	0.028	97.28	2.72	
	0.014	99.14	0.86	
$[Cu(L)H_2O]$	0.113	67.48	32.52	0.186
	0.057	82.38	17.62	
	0.028	97.28	2.72	
	0.014	99.14	0.86	
$[Mo(L)O_2\ (H_2O)]$	2.083	52.87	37.13	0.235
	1.042	60.03	39.97	
	0.521	68.34	31.66	
	0.260	77.65	22.35	

Conclusion

In summary, using a straightforward substitution process using 2-hydroxyquinoline, we were able to successfully synthesize a novel azo ligand derivative with 3-amino phenol. Then, ligand and metal complexes were identified using a variety of analytical methods, including thermal analysis (TGA and DSC) curves, elemental microanalysis, and metal-chloride containing, electrical conductivity measurement, magnetic susceptibility, ^{1}H and ^{13}CNMR, FT-IR, and UV-Vis spectra. Calculations of the thermodynamic parameters ΔH, ΔS, and ΔG were made using the DCS curve. The atomic N, O and O tridentate coordination sites in the ligand were identified by comparing their IR spectra to those of the metal complexes. The M:L ratio in every compound was [1:1]. The dye used the complexes prepared from it to determine their ability to inhibit free radicals by measuring their ability as antioxidants using DPPH as a free radical and ascorbic acid as a standard substance, and determining the value of IC_{50}, as it was found that the ligand had a high ability to inhibit free radicals, and the ability to inhibit the complexes varied according to the value of IC_{50}, and the results are follows (H_2L > Ascorbic acid > $[Cu(L)H_2O]$ > $[Mo(L)O_2(H_2O)]$ > $[Pt(L)H_2OCl_2]$ > $[Ni(L)H_2O]$ > $[Pd(L)H_2O]$).

Acknowledgment

Authors would like to thank everyone who contributed to the success of this review article Department of Chemistry, College of Science for Women, University of Baghdad, Ministry of Higher Education & Scientific Research & Science and Technology, Directorate of Environment & Water.

Authors' declaration

- Conflicts of Interest: None.
- We hereby confirm that all the Figures and Tables in the manuscript are ours. Furthermore, any Figures and images, that are not ours, have been included with the necessary permission for re-publication, which is attached to the manuscript.
- No animal studies are present in the manuscript.
- No human studies are present in the manuscript.
- Ethical Clearance: The project was approved by the local ethical committee at University of Baghdad.

Authors' contributions statement

F.Z.SH. conducted the practical side of the research, analysis of the results, and the writing of the manuscript. A. A. S. conceived the idea of the research, contributed in the analysis of the results and did the revision and the proofreading of the manuscript.

References

1. Mohammed H, Synthesis, identification, and biological study for some complexes of azo dye having theophylline. SciWorld J. 2021;2021:1–9. https://doi.org/10.1155/2021/9943763.
2. Mahmudov KT, Gurbanov AV, Aliyeva VA, Resnati G, Pombeiro AJ. Pnictogen bonding in coordination chemistry. CoordChem Rev. 2020;1(418):213381. https://doi.org/10.1016/j.ccr.2020.213381.
3. Manika R, Chavan VL. Thermal and antimicrobial studies of synthesized and characterized rhodium, platinum and gold metal complexes derived from (2E) N-(naphthalen-2yl)-3 phenyl prop-2en-1 imine schiff base. JSciRes. 2021;65(2):30–38. https://doi.org/10.37398/JSR.2021.650206.
4. Reda SM, Al-Hamdani AA. S.Mn (II), Fe (III), Co (II) and Rh (III) complexes with azo ligand: Synthesis, characterization, thermal analysis and bioactivity. Baghdad Sci J. 2023;20(3):642–660. https://dx.doi.org/10.21123/bsj.2022.7289.
5. Jain S, Dongare K, Nallamothu B, Dora CP, Kushwah V, Katiyar SS, *et al.* Enhanced stability and oral bioavailability of erlotinib by solid self nano emulsifying drug delivery systems. Int J Pharm. 2022;622:121852. https://doi.org/10.1016/j.ijpharm.2022.121852.
6. Parveen S. Recent advances in anticancer ruthenium Schiff base complexes. ApplOrganometalChem. 2020;34(8):e5687. https://doi.org/10.1002/aoc.5687.
7. Al-Hamdani AAS. Synthesis, Characterization, Thermal Studies, and Antioxidant Activities of Azo Dye [2-[(3-Hydroxyphenyl) diazinyl]-1, 2-Benzothiazol-3 (2H)-one-1, 1-Dioxide] and Metal Ion Complexes. Iraqi J. of Sci., 2024;65(12):6842–6861. https://doi.org/10.24996/ijs.2024.65.12.5.
8. Sudhakar C, Saravanabhavan M, Ramesh KS, Badavath VN, Chandrasekar S, Babu B, *et al.* Pharmacological and quantum chemical studies of 2-aminobenzo[d]thiazol-3-ium 4-chlorobenzenesulphonate. Synthesis, spectral, thermal analysis andstructural elucidation, Res Chem. 2022;4(100442):1–11. https://doi.org/10.1016/j.rechem.2022.100442.
9. Nakamoto K. Infrared and Raman Spectra of Inorganic and Coordination Compounds, Wiley-Inter Science: New York. 1997. https://doi.org/10.1002/9780470405840.
10. Reem GD, Walaa HM, Gehad GM. Metal complexes of tetradentateazo-dye ligand derived from 4, 4-oxydianiline: Preparation, structural investigation, biological evaluation and MOE studies. ApplOrganometal Chem. 2020;34(10):1–20. https://doi/10.1002/aoc.5883.
11. Ahmadi RA, Amani S. Synthesis, Spectroscopy, Thermal Analysis, Magnetic Properties and Biological Activity Studies of Cu(II) and Co(II) Complexes with Schiff Base Dye Ligands. Molecules. 2012;17(6):6434–6448. https://doi.org/10.3390/molecules17066434.
12. Mandour HS, Abouel-Enein SA, Morsi RM, Khorshed LA. Azo ligand as new corrosion inhibitor for copper metal: Spectral, thermal studies and electrical conductivity of its novel transition metal complexes. JMolStruct. 2021;5(1225):129159. https://doi.org/10.1016/j.molstruc.2020.129159.
13. Dahi MA, Jarad AJ. Synthesis, characterization and biological evaluation of thiazolyl azo ligand complexes with some metal ions. J Phys Conf Ser. 2020;1664(1):012090. https://doi.org/10.1088/1742-6596/1664/1/012090.
14. Sanaa ME, Saeyda AA, Fatma IA. Synthesis, spectral characterization, thermal studies and biological activity of (Z)-5-((1, 5-dimethyl-3-oxo-2-phenyl-2,3-dihydro-1H-pyrazol-4-yl)diazenyl)-6-hydroxy-2-mercaptopyrimidin-4(3H)-one and its metal complexes, ApplOrganometal Chem. 2018;32(5):e4073. https://doi.org/10.1002/aoc.4073.
15. Jaluddin SN, Zain ZM, Halim MIA, Safian MF, Rani MAA, Subri MSM. Preliminary Evaluation of Gunshot Residue (GSR) Using 3-Aminophenol as a Substitute in Modified Griess Test. IntJResPharm Sci. 2021;21(6):1550–1559. http://dx.doi.org/10.22146/ijc.68265.
16. Mandour HS, Abouel-Enein SA, Morsi RM, Khorshed LA. Azo ligand as new corrosion inhibitor for copper metal: Spectral, thermal studies and electrical conductivity of its novel transition metal complexes. JMol Struct. 2021;5(1225):129159. https://doi.org/10.1016/j.molstruc.2020.129159.
17. Geary WJ. The use of conductivity measurements in organic solvents for the characterisation of coordination compounds. Coord Chem Rev. 1971;7(1):81–122. https://doi.org/10.1016/S0010-8545(00)80009-0.
18. Refat MS, Alghool S, De Farias RF. Synthesis, Spectral, and Thermal Studies of Cu (II), Ni (II), Fe (III), and Sn (II) Complexes with Captopril Drug. Synth. ReactInorg. Met. 2010;40(9):585–591. https://doi.org/10.1080/15533174.2010.509295.
19. Abdulrazzaq AG, Al-Hamdani AAS. Some Metal Ions Complexes with Azo [4-((8-hydroxyquinolin-7-yl)-N(4-methylisoxazol-3-yl) benzene sulfon amide] Synthesis, Characterization, Thermal Study and Antioxidant Activity. JMed ChemSci. 2023;6(2):236–249. https://doi.org/10.26655/JMCHEMSCI.2023.2.7.
20. Hamza IS, Mahmmoud WA, Al-Hamdani AA, Ahmed SD, Allaf AW, Al Zoubi W. Synthesis, characterization, and bioactivity of several metalcomplexes of (4-Amino-N-(5-methyl-isaxazol-3-yl)-benzenesulfonamide). orgChemCommun. 2022;144:109776. https://doi.org/10.1016/j.inoche.2022.10977.
21. Ashrafuzzaman MD, Camellia FK, Mahmud AA, Pramanik MD, Nahar K, Haque M. Bioactive mixed ligand metal complexes of Cu (II), Ni (II), and Zn (II) ions: Synthesis, characterization, antimicrobial and antioxidant properties. JChilChemSoc. 2021;66(3):5295–9. http://dx.doi.org/10.4067/S0717-97072021000305295.
22. Baliyan S, Mukherjee R, Priyadarshini A, Vibhuti A, Gupta A, Pandey RP and Chang CM, Determination of antioxidants by DPPH radical scavenging activity and quantitative phytochemical analysis of Ficus religiosa. Molecules. 2022;27(4):1326. https://doi.org/10.3390/molecules27041326.
23. Ikechukwu PE, Peter AA. Synthesis, Characterization, Anticancer, and Antioxidant Studies of Ru(III) Complexes of Monobasic Tridentate Schiff Bases. Bioinorg Chem Appli. 2016;9672451:1–11. http://dx.doi.org/10.1155/2016/9672451.
24. Abd SS, Alkam HH, Al-Shemary RKR. Composition, depiction, antibacterial, antioxidant, and cytotoxicity activities studies of a new nano-sized binuclear metal (II) Schiff base complexes, AIP ConfProc. 2023;2414(1). https://doi.org/10.1063/5.0121776.
25. Saleh TA, Al-Samarrai RRH, Abdul-Razzaq NE. The antioxidant and antimicrobial activity for some new synthesized Schiff bases derived from Ascorbic acid. IntJRes Pharm.Sci. 2019;10(2):1510–1515. https://doi.org/10.26452/ijrps.v10i2.730.

26. Vhanale B, Kadam D, Shinde A. Synthesis, spectral studies, antioxidant and antibacterial evaluation of aromatic nitro and halogenated tetradentate Schiff bases. Heliyon. 2022;8(6):1–7. https://doi.org/10.1016/j.heliyon.2022.e09650.
27. El-Gammal OA, Mohamed FS, Rezk GN, El-Bindary AA. Synthesis, characterization, catalytic, DNA binding and antibacterial activities of Co (II), Ni (II) and Cu (II) complexes with new Schiff base ligand. JMol Liq. 2021;15(326):115223. https://doi.org/10.1016/j.molliq.2020.115223.
28. El-Gammal OA, El-Bindary AA, Mohamed FS, Rezk GN, El-Bindary MA. Synthesis, characterization, design, molecular docking, anti COVID-19 activity, DFT calculations of novel Schiff base with some transition metal complexes. J MolLiq. 2022;15(346):117850. https://doi.org/10.1016/j.molliq.2021.117850.
29. Khedr AM, El-Ghamry H, Kassem MA, Saad FA, El-Guesmi N. Novel series of nanosized mono-and homobi-nuclear metal complexes of sulfathiazole azo dye ligand: Synthesis, characterization, DNA-binding affinity, and anticancer activity. Inorg.ChemCommun. 2019;1(108):107496. https://doi.org/10.1016/j.inoche.2019.107496.
30. Al-Atbi HS, Al-Salami BK, Al-Assadi IJ. New azo-azomethine derivative of sulfanilamide: Synthesis, Characterization, Spectroscopic, Antimicrobial and Antioxidant activity study. JPhysConfSer. 2019;1294(5):r052033. https://doi.org/10.1088/1742-6596/1294/5/052033.

تحضير وتشخيص ودراسة أطياف الكتلة والتحلل الحراري لمعقدات بعض ايونات المعادن وتقييم فعاليتها كمضادات اكسدة

فاطمة الزهراء شاكر حاتم، عباس علي صالح الحمداني

قسم الكيمياء ،كلية العلوم للبنات ،جامعة بغداد ،بغداد ،العراق

الخلاصة

حضرت صبغة الازو الجديدة من تفاعل ملح الديازونيوم المشتق من 3- امينو فينول مع 2- هايدروكسي كوينولين ثم استخدم لتحضير سلسلة من المعقدات مع كلوريدات كل من الكوبلت والكروم والنحاس والنيكل والبلاتين والبلاديوموموليبدات الامونيوم، شخص الليكاند بطيف الرنين النووي المغناطيسي البروتوني والكاربوني كما شخص جمع المركبات المحضرة باطياف الاشعة تحت الحمراء وفوق البنفسجية – المرئية والكتلة فضلاً عن التحليل الحراري الوزني والمسعر التفاضلي والتحليل الدقيق للعناصر كما قيستالتوصيلية والحساسية المغناطيسية ومحتوى الفلز ومحتوى الكلور للمعقدات اوضحت النتائج ان الليكاند يسلك سلوك ثلاثي السن وضحت الصيغة المقترحة له وان المعقدات اعطت اشكال رباعية السطوحوثمانيه السطوح عدا البلاديوم اعطى مربع مستوي كما اظهرت النتائج احتواء المعقدات على الماء داخل مجال التناسق وان جميعها غير الكتروليتية . استخدم الصبغة المعقدات المحضرة منها لتحدد قابليتها على كبح الجذور الحرة من خلال قياس قابليتها كمضادات اكسدة باستخدام مادة DPPH كجذر حر وحامض الاسكوربك كمادة قياسية وتحديد قيمة IC_{50} حيث وجد ان الليكاند يمتلك قابلية عالية على كبح الجذور الحرة والمعقدات تفاوتت قابليتها على الكبح حسب قيمة IC_{50} وكانت النتائج كما يلي:

(H_2L > Ascorbic acid >Cu-complex >Mo-complex > Pt-complex >Ni-complex > Pd-complex)

الكلمات المفتاحية: مضادات الأكسدة، معقدات الآزو، 3-أمينوفينول، 2-هيدروكسي كينولين، الثوابت الديناميكية الحرارية